Diabetologia (2017) 60:336–345
DOI 10.1007/s00125-016-4151-9

ARTICLE

A *Tbc1d1*^{Ser231Ala}-knockin mutation partially impairs AICAR- but not exercise-induced muscle glucose uptake in mice

Qiaoli Chen[1] · Bingxian Xie[1] · Sangsang Zhu[1] · Ping Rong[1] · Yang Sheng[1] · Serge Ducommun[2] · Liang Chen[1] · Chao Quan[1] · Min Li[1] · Kei Sakamoto[2] · Carol MacKintosh[3] · Shuai Chen[1,4] · Hong Yu Wang[1,4]

Received: 28 July 2016 / Accepted: 14 October 2016 / Published online: 8 November 2016

Abstract

Aims/hypothesis TBC1D1 (tre-2/USP6, BUB2, cdc16 domain family member 1) is a Rab GTPase-activating protein (RabGAP) that has been implicated in regulating GLUT4 trafficking. TBC1D1 can be phosphorylated by the AMP-activated protein kinase (AMPK) on Ser^{231}, which consequently interacts with 14-3-3 proteins. Given the key role for AMPK in regulating insulin-independent muscle glucose uptake, we hypothesised that TBC1D1-Ser^{231} phosphorylation and/or 14-3-3 binding may mediate AMPK-governed glucose homeostasis.

Methods Whole-body glucose homeostasis and muscle glucose uptake were assayed in mice bearing a *Tbc1d1*^{Ser231Ala}-knockin mutation or harbouring skeletal muscle-specific *Ampkα1*/*α2* (also known as *Prkaa1*/2) double-knockout mutations in response to an AMPK-activating agent, 5-aminoimidazole-4-carboxamide-1-β-D-ribofuranoside (AICAR). Exercise-induced muscle glucose uptake and exercise capacity were also determined in the *Tbc1d1*^{Ser231Ala}-knockin mice.

Results Skeletal muscle-specific deletion of *Ampkα1*/*a2* in mice prevented AICAR-induced hypoglycaemia and muscle glucose uptake. The *Tbc1d1*^{Ser231Ala}-knockin mutation also attenuated the glucose-lowering effect of AICAR in mice. Glucose uptake and cell surface GLUT4 content were significantly lower in muscle isolated from the *Tbc1d1*^{Ser231Ala}-knockin mice upon stimulation with a submaximal dose of AICAR. However, this *Tbc1d1*^{Ser231Ala}-knockin mutation neither impaired exercise-induced muscle glucose uptake nor affected exercise capacity in mice.

Conclusions/interpretation TBC1D1-Ser^{231} phosphorylation and/or 14-3-3 binding partially mediates AMPK-governed glucose homeostasis and muscle glucose uptake in a context-dependent manner.

Keywords 14-3-3 · AMPK · Glucose uptake · Phosphorylation · TBC1D1

Qiaoli Chen and Bingxian Xie contributed equally to this study.

Shuai Chen and Hong Yu Wang are joint senior authors.

Electronic supplementary material The online version of this article (doi:10.1007/s00125-016-4151-9) contains peer-reviewed but unedited supplementary material, which is available to authorised users.

✉ Shuai Chen
schen6@163.com

✉ Hong Yu Wang
wanghy@nicemice.cn

[1] MOE Key Laboratory of Model Animal for Disease Study and State Key Laboratory of Pharmaceutical Biotechnology, Model Animal Research Center, Nanjing Biomedical Research Institute, Nanjing University, Pukou District, Nanjing 210061, China

[2] Nestlé Institute of Health Sciences SA, Campus EPFL, Quartier de l'Innovation, Bâtiment G, Lausanne, Switzerland

[3] Division of Cell and Developmental Biology, School of Life Sciences, University of Dundee, Dundee, Scotland, UK

[4] Collaborative Innovation Center of Genetics and Development, Shanghai, China

Abbreviations

ACC	Acetyl-CoA carboxylase
AICAR	5-Aminoimidazole-4-carboxamide-1-β-D-ribofuranoside
AMPK	AMP-activated protein kinase
Ampkα1/*α2*-mKO	Skeletal muscle-specific *Ampkα1*/*α2*-knockout
AS160	Akt substrate of 160 kDa
EDL	Extensor digitorum longus

GAP	GTPase-activating protein
GEF	Guanine nucleotide exchange factor
PKB	Protein kinase B
RabGAP	Rab GTPase-activating protein
TBC1D1	Tre-2/USP6, BUB2, cdc16 domain family member 1

Introduction

Type 2 diabetes has become pandemic in the last few decades, which urges novel therapeutics to prevent, treat or cure the disease. As insulin sensitivity is generally decreased in type 2 diabetic patients, insulin-independent treatment is commonly considered to combat type 2 diabetes. The energy sensor AMP-activated protein kinase (AMPK) has been proposed as an attractive drug target for treatment of type 2 diabetes as its activation brings about many of the acute and chronic beneficial effects of exercise and promotes muscle glucose uptake in an insulin-independent mechanism [1, 2].

The heterotrimeric AMPK holoenzyme consists of a catalytic subunit α (α1 and α2), a regulatory subunit γ (γ1, γ2 and γ3) and a third subunit β (β1 and β2) that bridges the α and γ subunits [1]. AMPK regulates whole-body glucose homeostasis by various mechanisms [1, 3, 4], one of which is control of muscle glucose uptake by promoting translocation of GLUT4 from its intracellular storage sites onto plasma membrane [5]. Whole-body deletion of the AMPK α2 or β2 subunit, or overexpression of a dominant inhibitory mutant of AMPK in muscle, attenuates the hypoglycaemic effect of AICAR in mice. Furthermore, genetic inactivation of the AMPK α2, β2 or γ3 subunit, or overexpression of the dominant inhibitory mutant of AMPK, inhibits AICAR-stimulated muscle glucose uptake [6–10]. However, the regulatory mechanism of AMPK-dependent GLUT4 translocation remains to be elucidated. GLUT4 also mediates insulin-stimulated glucose uptake into skeletal muscle and adipose, in which translocation in response to insulin is regulated by the protein kinase B (PKB, also known as Akt) pathway [11].

Two related Rab GTPase-activating proteins (RabGAPs), Akt substrate of 160 kDa (AS160, also known as TBC1D4) and tre-2/USP6, BUB2, cdc16 domain family member 1 (TBC1D1), have been linked with type 2 diabetes and obesity, respectively [12–15]. These enzymes have also been implicated in regulating GLUT4 trafficking (reviewed by Sakamoto and Holman [16]). Both AS160 and TBC1D1 can be phosphorylated on multiple sites by protein kinases including PKB and AMPK (reviewed by Chen et al [17]). Overexpression of an AS160-4P mutant (in which Ser^{325}, Ser^{595}, Thr^{649} and Ser^{758} were replaced by alanine) or a TBC1D1-3P mutant (in which alanine replaced Ser^{489}, Thr^{499}/Ser^{501} and Thr^{590}) robustly inhibits insulin-stimulated GLUT4 translocation in 3T3-L1 adipocytes [18, 19]. In contrast, overexpression of a TBC1D1-4P mutant (in which alanine replaced Ser^{231}, Thr^{499}, Thr^{590} and Ser^{621}) decreases contraction-induced glucose uptake in mouse skeletal muscle [20]. Upon phosphorylation, both AS160 and TBC1D1 bind to regulatory 14-3-3 proteins (reviewed by Chen et al [17]). The AS160−14-3-3 interaction is regulated by insulin and mainly mediated by phosphorylated Thr^{649} on AS160 [21, 22], whereas 14-3-3 binding to TBC1D1 depends on AMPK and mainly requires phosphorylated Ser^{231} on TBC1D1 [23, 24]. Moreover, 14-3-3 binding to AS160 has been implicated in participating insulin-stimulated GLUT4 translocation in 3T3-L1 adipocytes [21]. On the basis of these findings, we put forward a hypothesis that AS160−14-3-3 interaction is required for insulin-stimulated GLUT4 trafficking and glucose homeostasis, while 14-3-3 binding to TBC1D1 mediates AMPK-dependent GLUT4 translocation and glucose homeostasis [17]. Towards addressing this hypothesis, we previously generated an *As160*^{Thr649Ala}-knockin mouse model in which insulin-induced AS160-Thr^{649} phosphorylation and its binding to 14-3-3s was prevented, and showed that the *As160*^{Thr649Ala}-knockin mice exhibited insulin resistance mainly through impaired GLUT4 translocation and glucose uptake into skeletal muscle in response to insulin [25]. In contrast, AICAR-stimulated muscle glucose uptake and hypoglycaemia, which are independent of insulin, were normal in these mice [26].

In this study, we used a recently reported *Tbc1d1*^{Ser231Ala}-knockin mouse model in which the knockin mutation prevents AMPK-dependent phosphorylation of TBC1D1-Ser^{231} [27] to further test the above hypothesis.

Methods

Materials Recombinant human insulin was bought from Novo Nordisk (Bagsvaerd, Denmark) and AICAR from Toronto Research Chemicals (Toronto, ON, Canada). Protein G-Sepharose was from GE Healthcare (Little Chalfont, UK). 2-deoxy-D-[1,2-^{3}H(*N*)]glucose and D-1-[^{14}C]mannitol were from PerkinElmer (American Fork, UT, USA). All other chemicals were from Sigma-Aldrich (Shanghai, China) or Sangon Biotech (Shanghai, China). Total TBC1D1 antibody is as previously described [23]. The commercial antibodies are listed in electronic supplementary material (ESM) Table 1.

Mouse breeding and genotyping The Ethics Committees, initially at the University of Dundee and latterly at Nanjing University, approved all animal protocols. Mice were kept under a light/dark cycle of 12 h. Animal experiments were not carried out in a blinded or randomised manner. The *Tbc1d1*^{Ser231Ala}-knockin mice were generated at the University of Dundee as previously described [27]. The *Ampkα1*$^{f/f}$ and *Ampkα2*$^{f/f}$ mice were as previously described [28], and obtained from the Jackson Laboratory (Bar Harbor,

ME, USA). They were mated with each other to obtain *Ampkα1/α2*$^{f/f}$ mice. The *Ampkα1/α2*$^{f/f}$ mice were then mated with the Myf5-Cre mice [29] to obtain the *Ampkα1/α2*$^{f/f}$–*Myf5*-Cre mice that are the skeletal muscle-specific *Ampkα1/α2*-knockout (*Ampkα1/α2*-mKO) mice. Genotyping was carried out using primers listed in ESM Table 2.

Tissue lysis, immunoprecipitation, immunoblotting and 14-3-3 overlay Homogenisation of mouse tissues and protein concentration measurement were carried out as previously described [26].

Immunoprecipitation of TBC1D1 protein, immunoblotting and 14-3-3 overlay were carried out as previously described [23].

AICAR tolerance and insulin tolerance tests Mice were partially fasted for 4 h prior to AICAR or insulin tolerance test. Afterwards, basal blood glucose was measured using a Breeze 2 glucometer (Bayer, Leverkusen, Germany) via tail bleeding. Mice were intraperitoneally injected with AICAR (0.25 mg/g) for AICAR tolerance tests or insulin (0.75 mU/g) for insulin tolerance tests. After injection of AICAR or insulin, blood glucose levels were measured at the indicated time intervals.

Muscle incubation, glucose uptake and photolabelling of cell surface GLUT4 in isolated muscle Muscle isolation and glucose uptake assays were carried out as previously described [25]. Briefly, isolated muscles were incubated in KRB (± AICAR) for 50 min. For biochemistry studies, muscles were then blotted dry and snap frozen in liquid nitrogen for subsequent analysis. For glucose uptake, muscles were further incubated in KRB (± AICAR) containing 2-deoxy-D-[1,2-^{3}H(*N*)]glucose and D-1-[^{14}C]mannitol for 10 min. Radioisotopes in muscle lysates were determined using a Tri-Carb 2800TR scintillation counter (PerkinElmer). For the photolabelling experiment, cell surface GLUT4 in isolated extensor digitorum longus (EDL) muscle was chemically tagged with the photolabel Bio-LC-ATB-BGPA and quantified as previously described [25].

Treadmill exercise Two types of treadmill running tests, a power test (short high-intensity run) and an endurance test (long low-intensity run), were performed to assess maximal exercise performance in mice using a treadmill (Techman Soft, Chengdu, China) as previously described [30]. Briefly, mice were acclimated to treadmill running (5 min per day at 15 cm/s, +5° slope and 0.3 mA electrical stimulation) for 5 days before the tests. For power tests, the treadmill was set with a +5° slope and 0.3 mA aversive electrical stimulation. Belt speed was set at 15 cm/s initially and increased by 2 cm/s every minute. As for endurance tests, the treadmill was set with a +5° slope and 0.3 mA aversive electrical stimulation. Belt speed was set at 15 cm/s initially and increased by 3 cm/s every 12 min. Running tests were terminated when mice failed to re-engage on the treadmill despite aversive stimulation for more than 15 s.

Exercise-stimulated muscle glucose uptake in vivo Exercise-stimulated muscle glucose uptake was carried out as previously described [31]. Briefly, mice were intraperitoneally injected with 3.7×10^5 Becquerel (Bq) of 2-deoxy-D-[1,2-^{3}H(*N*)]glucose immediately prior to rest or exercise. For the exercise group, mice were subjected to 35 min of treadmill running (30 cm/s belt speed, +10° slope). For the resting group, mice were kept in home cages for 35 min. After exercise or rest, mice were euthanised and gastrocnemius and quadriceps muscles were harvested for further analysis. An assumption was made that systemic delivery of the tracer was similar in all animals within each experimental group as the appearance of 2-deoxy-D-[1,2-^{3}H(*N*)]glucose in the blood was not determined for technical reasons. Muscle accumulation of phosphorylated 2-deoxy-D-[1,2-^{3}H(*N*)]glucose was determined and used for calculation of in vivo muscle glucose-uptake rates as previously described [25].

Histology and imaging Isolated soleus and EDL muscles were embedded in tissue freezing medium (14020108926, Leica, Mannheim, Germany), frozen in liquid nitrogen and sectioned using a Leica RM2016 microtome. Muscle fibre type (I, IIa, and IIb/IIx) in soleus and EDL muscle was determined using myosin ATPase staining as previously described [32]. After staining, pictures were taken on sections using an Olympus BX53F microscope (Tokyo, Japan).

Immunofluorescence staining and imaging Immunofluorescence staining of GLUT4 was performed in single muscle fibres as previously described [27]. Images were photographed using a Leica confocal microscope.

Statistical analysis Data are given as mean ± SEM. Two-group comparisons were carried out using Student's *t* test, and multiple-group comparisons were performed with two-way ANOVA using Prism software (GraphPad, San Diego, CA, USA). Differences were considered statistically significant at $p < 0.05$.

Results

Deletion of *Ampkα1/α2* in skeletal muscle blunted the hypoglycaemic effect of AICAR and AICAR-stimulated muscle glucose uptake It has been shown that overexpression of the dominant inhibitory mutant of AMPK in skeletal and cardiac muscle attenuates AICAR-induced hypoglycaemia [9]. To further determine the contribution of skeletal muscle AMPK to AICAR-induced hypoglycaemia, we generated an

Ampkα1/α2-mKO mouse model in which both AMPK α1 and α2 subunits were specifically deleted in skeletal muscle. Deletion of AMPK α1 and α2 subunits caused a substantial decrease in TBC1D1-Ser^{231} phosphorylation but did not alter expression of TBC1D1 and AS160 in skeletal muscle (Fig. 1a). Expression and phosphorylation of AMPKα and TBC1D1 remained normal in other tissues analysed (Fig. 1b, c). Intraperitoneal injection of AICAR caused hypoglycaemia in the *Ampkα1/α2*$^{f/f}$ control mice (Fig. 1d). Interestingly, this hypoglycaemic effect of AICAR was blunted in the *Ampkα1/α2*-mKO mice (Fig. 1d). As expected, glucose uptake was completely inhibited in the AMPKα1/α2-deficient soleus and EDL muscle in response to AICAR (2 mmol/l) (Fig. 1e, f). Concomitantly, AICAR-stimulated GLUT4 translocation was impaired in EDL muscle from the *Ampkα1/α2*-mKO mice (Fig. 1g, h). These data confirm previous reports that AMPK controls AICAR-stimulated muscle glucose uptake and GLUT4 translocation [6–10, 33], and also demonstrate that muscle AMPK makes a large, if not complete, contribution to AICAR-induced hypoglycaemia under the conditions used in this study.

The *Tbc1d1*^{Ser231Ala}-knockin mutation attenuated the hypoglycaemic effect of AICAR Next, we employed the *Tbc1d1*^{Ser231Ala}-knockin mice to investigate whether TBC1D1 mediates the AICAR-induced hypoglycaemic effect downstream of AMPK. Intraperitoneal injection of AICAR induced phosphorylation of AMPK and a well-established bone fide AMPK substrate acetyl-CoA carboxylase (ACC) in knockin muscle to a similar extent as in wild-type (WT) muscle (Fig. 2a). In contrast and as anticipated, AICAR-stimulated TBC1D1-Ser^{231} phosphorylation was detected only in muscle extracts from the WT mice but not knockins (Fig. 2a). The AICAR-stimulated 14-3-3−TBC1D1 interaction assessed by a 14-3-3 overlay assay was also pronouncedly reduced (by over 80%) in TBC1D1 immunoprecipitates from the knockin muscle extracts compared with the WT controls (Fig. 2a). As previously reported [27], expression of

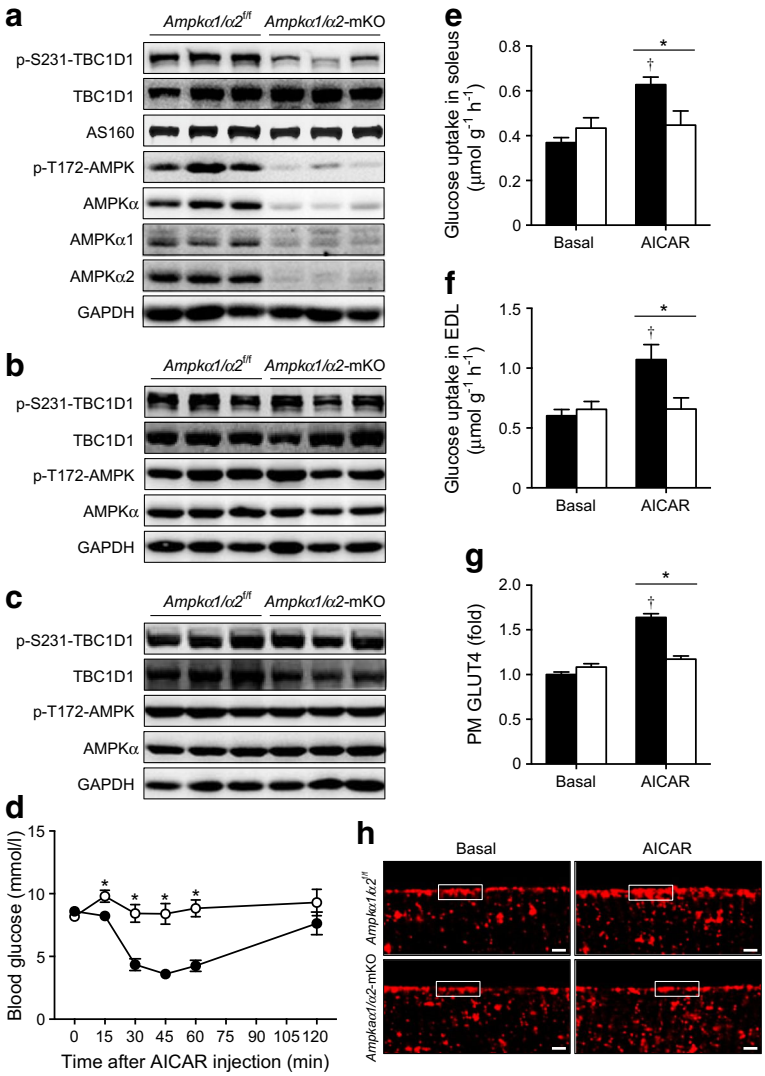

Fig. 1 AICAR-stimulated glucose clearance and muscle glucose uptake in *Ampkα1/α2*-mKO mice. (**a**–**c**) Expression and phosphorylation of TBC1D1, AS160 and AMPKα in skeletal muscle (**a**), heart (**b**) and liver (**c**). (**d**) AICAR tolerance test of male *Ampkα1/α2*$^{f/f}$ and *Ampkα1/α2*-mKO mice (6–8 weeks old); $n = 5$–6. (**e**) Glucose uptake in soleus muscle ex vivo in response to AICAR (2 mmol/l); $n = 7$. (**f**) Glucose uptake in EDL muscle ex vivo in response to AICAR (2 mmol/l). $n = 5$–6. (**g**, **h**) GLUT4 staining in EDL muscle fibres in response to AICAR (2 mmol/l). (**g**) GLUT4 content of the plasma membrane. (**h**) Representative images from the experiment. At least 100 bracketed regions (examples shown in **h**) from ~20 muscle fibres were quantified per condition/genotype. Scale bars, 2 μm. Statistical analyses were performed using the *t* test for (**d**) or two-way ANOVA for (**e**–**g**). *$p < 0.05$; †$p < 0.05$ (*Ampkα1/α2*$^{f/f}$ AICAR vs *Ampkα1/α2*$^{f/f}$ basal). Black bars/symbols, *Ampkα1/α2*$^{f/f}$; white bars/symbols, *Ampkα1/α2*-mKO. GAPDH, glyceraldehyde 3-phosphate dehydrogenase; PM, plasma membrane

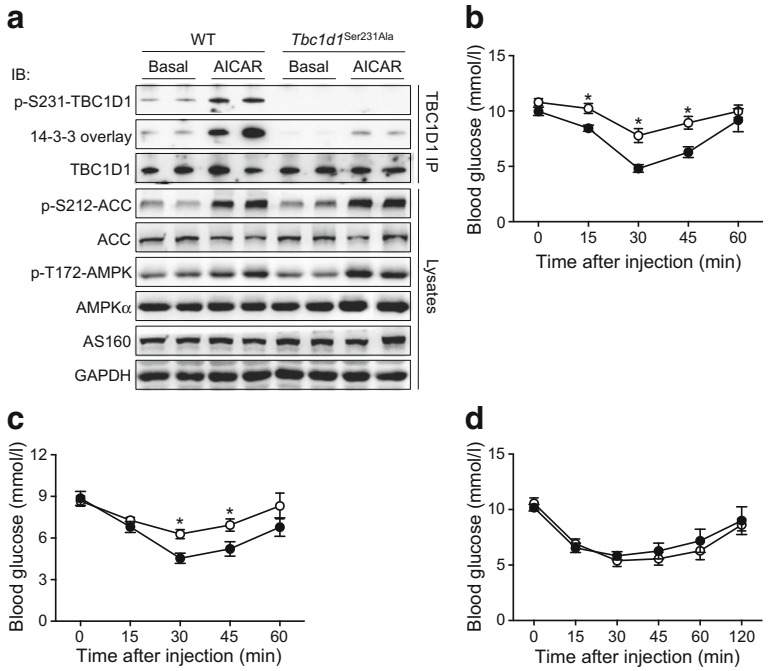

Fig. 2 Glucose clearance in the *Tbc1d1*^{Ser231Ala}-knockin mice after intraperitoneal injection with AICAR or insulin. (**a**) Ser^{231} phosphorylation and 14-3-3 binding of TBC1D1 in skeletal muscle on AICAR stimulation. TBC1D1 protein was immunoprecipitated from lysates of TA muscle from mice injected intraperitoneally with either saline (154 mmol/l NaCl; basal) or AICAR (0.25 mg/g), and immunoblotted. Total and phosphorylated ACC, AMPK and AS160 were measured in muscle lysates with glyceraldehyde 3-phosphate dehydrogenase (GAPDH) as internal control. (**b**) AICAR tolerance test of male mice at 6–8 weeks of age. $n = 9$–12. (**c**) AICAR tolerance test of female mice at 6–8 weeks of age. $n = 6$. (**d**) Insulin tolerance test of male mice at 10–12 weeks of age. $n = 6$–7. Statistical analyses were carried out using the *t* test. $^*p < 0.05$ vs WT. White symbols, *Tbc1d1*^{Ser231Ala}; black symbols, wild type. IB, immunoblot; IP, immunoprecipitate

AS160 remained normal in *Tbc1d1*^{Ser231Ala}-knockin muscle (Fig. 2a). Interestingly, the hypoglycaemic effect of AICAR was significantly attenuated in both male and female *Tbc1d1*^{Ser231Ala}-knockin mice (6–8 weeks old) (Fig. 2b, c). We previously showed that the *Tbc1d1*^{Ser231Ala}-knockin mice were tolerant to glucose administration at a young age (less than 4 months old) [27]. In agreement with this report, insulin injection lowered blood glucose levels to a similar extent in the young *Tbc1d1*^{Ser231Ala}-knockin mice and WT littermates (10–12 weeks old) (Fig. 2d).

AICAR-stimulated glucose uptake was decreased in skeletal muscle from the *Tbc1d1*^{Ser231Ala}-knockin mice We first examined whether soleus and EDL muscles exhibit different sensitivity to AICAR in the glucose uptake assay as they have different fibre compositions. To this end, two concentrations of AICAR were used to stimulate glucose uptake in WT soleus and EDL muscles. Glucose-uptake rates stimulated by a low concentration of AICAR (0.25 mmol/l) were ~55% and ~94% of those stimulated by the high concentration of AICAR (2 mmol/l) in soleus and EDL muscles, respectively (Fig. 3a), suggesting that EDL muscle is more sensitive to AICAR treatment.

We next investigated whether the *Tbc1d1*^{Ser231Ala}-knockin mutation impaired AICAR-stimulated muscle glucose uptake. Glucose uptake was normal in soleus and EDL muscles from the *Tbc1d1*^{Ser231Ala}-knockin mice under basal conditions. Upon stimulation with AICAR (2 mmol/l), glucose-uptake rates in the knockin soleus muscle were nearly 20% lower ($p = 0.0501$) than those in the WT muscle (Fig. 3b). Upon stimulation with the high concentration of AICAR (2 mmol/l), glucose-uptake rates were only marginally lower (not statistically significant) in the knockin EDL muscle than in the WT muscle (Fig. 3c). Interestingly, upon stimulation with a low concentration of AICAR (0.15 mmol/l), glucose uptake rates in the knockin EDL muscle were significantly lower, by ~17%, than those in the WT muscle (Fig. 3c). These data show that the *Tbc1d1*^{Ser231Ala}-knockin mutation moderately impaired AICAR-stimulated muscle glucose uptake.

Fibre composition of both soleus and EDL muscles from the *Tbc1d1*^{Ser231Ala}-knockin mice had no obvious differences compared with the corresponding muscles from the WT littermates (Fig. 4a–c), indicating that muscle fibre type switch is not the cause of impaired AICAR-stimulated glucose uptake in skeletal muscle from the *Tbc1d1*^{Ser231Ala}-knockin mice.

AICAR-stimulated GLUT4 translocation was impaired in EDL muscle from the *Tbc1d1*^{Ser231Ala}-knockin mice GLUT4 is the major glucose transporter that mediates AICAR-stimulated glucose uptake and it undergoes subcellular translocation to the plasma membrane on AICAR stimulation [9]. As previously reported [27], GLUT4 expression was

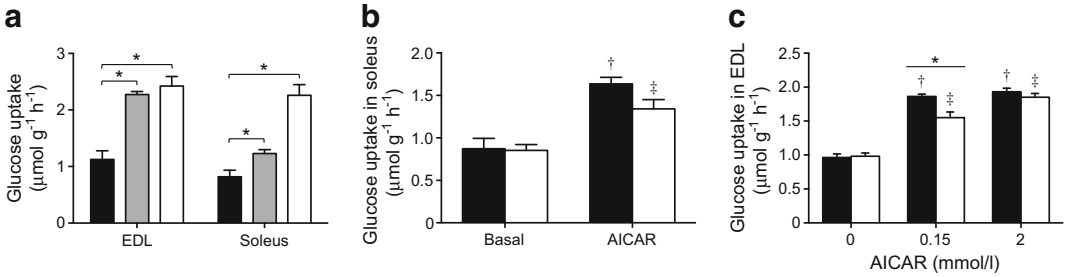

Fig. 3 Glucose uptake in skeletal muscle ex vivo on AICAR stimulation. (**a**) Glucose uptake in EDL and soleus muscle ex vivo in response to AICAR (0.25 mmol/l and 2 mmol/l). $n = 4$. Black bars, no AICAR; grey bars, 0.25 mmol/l AICAR; white bars, 2 mmol/l AICAR. $^{*}p < 0.05$ as shown. (**b**) Glucose uptake in soleus muscle ex vivo in response to AICAR (2 mmol/l). $n = 6$–7. $^{\dagger}p < 0.05$ (WT AICAR vs WT basal); $^{\ddagger}p < 0.05$ (*Tbc1d1*^{Ser231Ala} AICAR vs *Tbc1d1*^{Ser231Ala} basal). $p = 0.0501$ (WT AICAR vs *Tbc1d1*^{Ser231Ala} AICAR). (**c**) Glucose uptake in EDL muscle ex vivo in response to AICAR (0.15 mmol/l and 2 mmol/l). $n = 15$–21. $^{*}p < 0.05$ as shown. $^{\dagger}p < 0.05$ (WT AICAR vs WT basal); $^{\ddagger}p < 0.05$ (*Tbc1d1*^{Ser231Ala} AICAR vs *Tbc1d1*^{Ser231Ala} basal). Statistical analyses were performed using the *t* test for (**a**) or two-way ANOVA for (**b**, **c**). In (**b**, **c**) black bars, WT; white bars, *Tbc1d1*^{Ser231Ala}

normal in EDL muscle from the *Tbc1d1*^{Ser231Ala}-knockin mice (Fig. 5a, b). However, the GLUT4 content of the cell surface determined using a photolabelling method was increased by only ~25% in ex vivo EDL muscle from the *Tbc1d1*^{Ser231Ala}-knockin mice upon stimulation with 0.15 mmol/l AICAR, in contrast to an increase of ~53% in WT control muscle (Fig. 5c), suggesting that defects in GLUT4 translocation underlie the impaired glucose transport in skeletal muscle from the *Tbc1d1*^{Ser231Ala}-knockin mice. We also confirmed that AICAR increased phosphorylation of AMPK and ACC in ex vivo EDL muscle from both genotypes to similar extents (Fig. 5a). As expected, AICAR stimulated TBC1D1-Ser^{231} phosphorylation in ex vivo EDL muscle from the WT mice but not from the *Tbc1d1*^{Ser231Ala}-knockins (Fig. 5a).

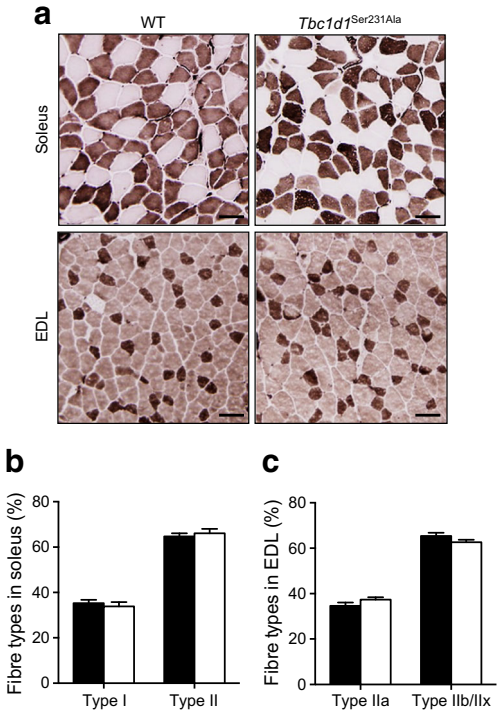

Fig. 4 Muscle fibre composition in soleus and EDL muscles from the WT and *Tbc1d1*^{Ser231Ala}-knockin mice. (**a**) Representative images of myosin ATPase staining in soleus and EDL muscle for determination of muscle fibre composition. Scale bars, 50 μm. (**b**, **c**). Percentage of different muscle fibres in soleus (**b**) and EDL (**c**) muscle. Soleus, $n = 4$–5; EDL, $n = 5$–7. Statistical analyses were performed using the *t* test. Black bars, WT; white bars, *Tbc1d1*^{Ser231Ala}

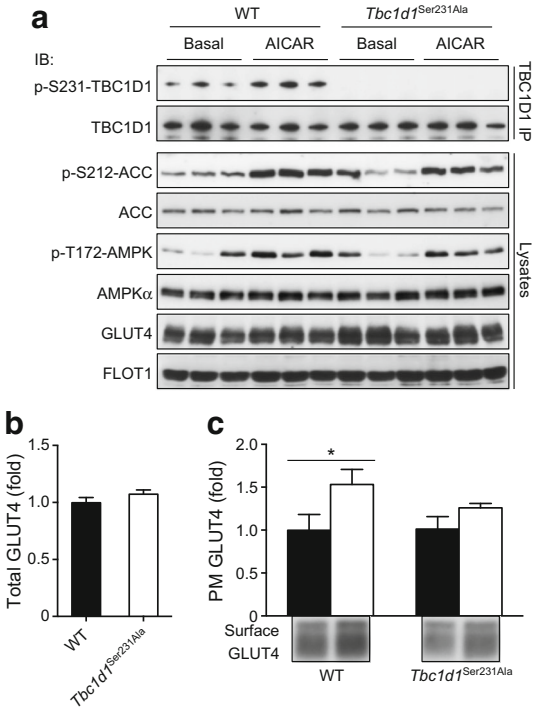

Fig. 5 Cell surface GLUT4 content in EDL muscle ex vivo on AICAR stimulation. (**a**) Expression and phosphorylation of TBC1D1, ACC and AMPK, and expression of GLUT4 in EDL muscle ex vivo on AICAR stimulation. Phosphorylation of TBC1D1-Ser^{231} was measured on immunoprecipitated TBC1D1 protein. (**b**) Quantification of GLUT4 protein in EDL muscle. The GLUT4 blot from Fig. 5a was used for quantification. $n = 6$. (**c**) Cell surface GLUT4 levels in EDL muscle ex vivo in response to AICAR (0.15 mmol/l). $n = 4$. Representative blots are shown. Statistical analyses were performed using *t* test for (**b**) or two-way ANOVA for (**c**); $^{*}p < 0.05$. Black bars, basal; white bars, AICAR. FLOT1, flotillin 1; IB, immunoblot; PM, plasma membrane

The *Tbc1d1*^{Ser231Ala}-knockin mutation did not impair exercise performance or exercise-induced muscle glucose uptake in mice It has been well established that AMPK regulates exercise performance and exercise-induced muscle glucose uptake [34]. We sought to find whether TBC1D1-Ser^{231} phosphorylation might mediate these effects of AMPK. The *Tbc1d1*^{Ser231Ala}-knockin mice displayed normal exercise performance in both power and endurance running tests (Fig. 6a–d). Phosphorylation of AMPK and ACC was increased in the exercised muscle from both genotypes to similar extents (Fig. 6e). In contrast, phosphorylation of TBC1D1-Ser^{231} was increased only in the exercised muscle from WT mice, and not that from *Tbc1d1*^{Ser231Ala}-knockins (Fig. 6e). Exercise robustly increased muscle glucose uptake, which was comparable in skeletal muscle from the *Tbc1d1*^{Ser231Ala}-knockin mice and WT littermates (Fig. 6f, g). The unaltered exercise-induced muscle glucose uptake was consistent with the recently reported normal contraction-stimulated glucose uptake in skeletal muscle from the *Tbc1d1*^{Ser231Ala}-knockin mice [27].

Discussion

Here we employed the *Tbc1d1*^{Ser231Ala}-knockin mouse to study the in vivo function of TBC1D1-Ser^{231} phosphorylation and its subsequent 14-3-3 binding in mediating AMPK-governed muscle glucose uptake. A major finding of this study is that TBC1D1-Ser^{231} phosphorylation and/or its binding to 14-3-3s regulates AICAR-mediated glucose metabolism at both peripheral and whole-body levels downstream of AMPK.

AICAR is widely used as a tool compound to study AMPK signalling, and it lowers blood glucose in an AMPK-dependent manner when administered to mice. Overexpression of a kinase-dead mutant form of AMPKα2 or genetic ablation of AMPK α2 or β2 can attenuate the hypoglycaemic effect of AICAR [6–9]. The contribution of AMPK to AICAR-induced hypoglycaemia in various organs may depend on the fasting status of mice. For instance, our data demonstrate that muscle AMPK makes a large, if not complete, contribution to AICAR-induced hypoglycaemia in mice subjected to partial fasting for 4 h. This hypoglycaemic effect is most likely caused by AICAR-stimulated glucose uptake in skeletal muscle, which is blunted in the *Ampkα1/α2*-mKO mice. However, in overnight-fasted mice, liver AMPK also partially mediates AICAR-induced hypoglycaemia [35]. Our *Tbc1d1*^{Ser231Ala}-knockin mouse is a whole-body knockin model, which has more lean mass and normal fat mass at a young age (less than 4 months old) [27]. Even though skeletal muscle plays a dominant role in AICAR-induced hypoglycaemia in mice subjected to partial fasting (4 h), it is still possible that the *Tbc1d1*^{Ser231Ala}-knockin mutation might impair AICAR-induced hypoglycaemia through multiple organs including skeletal muscle. The *Tbc1d1*^{Ser231Ala}-knockin mice have higher plasma IGF1 levels that activate the protein kinase B (PKB) pathway in skeletal muscle. Consequently, the PKB activates the downstream mTOR pathway, but does not phosphorylate AS160, which is a key regulator for muscle glucose uptake [27]. Currently, we do not know whether IGF1 levels can affect AICAR-induced hypoglycaemia in mice.

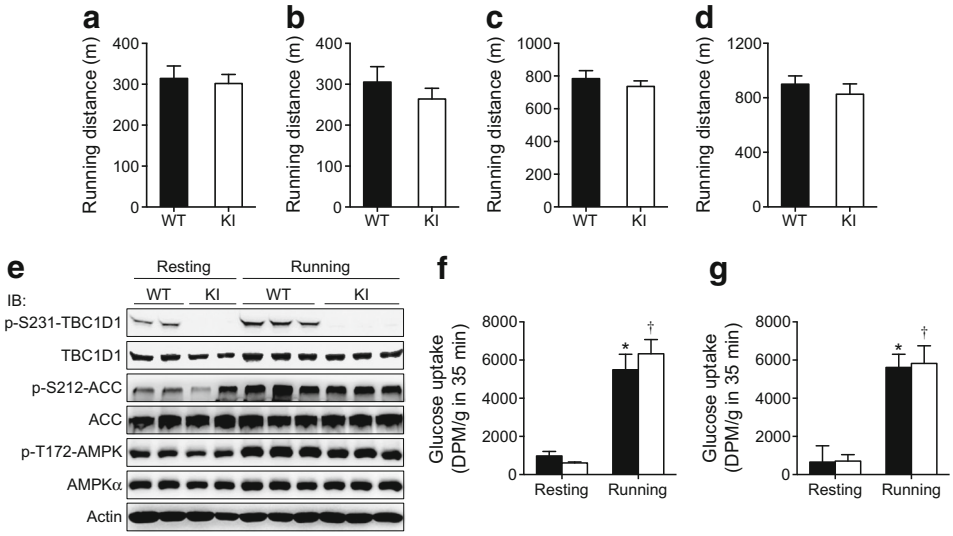

Fig. 6 Exercise performance and exercise-stimulated muscle glucose uptake in vivo. (**a**–**d**) Treadmill running exercise in the WT and *Tbc1d1*^{Ser231Ala} mice (3 months old). Power test in (**a**) male and (**b**) female mice. Endurance test in (**c**) male and (**d**) female mice; $n = 6$–15. (**e**) Total and phosphorylated TBC1D1, ACC and AMPK in gastrocnemius muscle from rested or treadmill-exercised mice (female mice, 7–8 weeks old). (**f**, **g**) In vivo muscle glucose uptake in gastrocnemius (**f**) and quadriceps (**g**) from rested or treadmill-exercised WT and *Tbc1d1*^{Ser231Ala} mice (female mice, 7–8 weeks old). Resting group, $n = 3$–5; running group, $n = 6$–7. *$p < 0.05$ (WT running vs WT resting); †$p < 0.05$ (*Tbc1d1*^{Ser231Ala} running vs *Tbc1d1*^{Ser231Ala} resting). Statistical analyses were performed using *t* test for (**a**–**d**) or two-way ANOVA for (**f**, **g**). Black bars, WT; white bars, *Tbc1d1*^{Ser231Ala}. DPM, disintegrations per min; KI, *Tbc1d1*^{Ser231Ala} knockin; IB, immunoblot

It is worth noting that the *Ampkα1/α2*-mKO mice were completely resistant to the hypoglycaemic effect of AICAR, and glucose uptake was blunted in isolated skeletal muscle from our *Ampkα1/α2*-mKO mice (this study) and other AMPK mouse models, even with the high concentration of AICAR (2 mmol/l) [6–10]. In contrast, the *Tbc1d1*^{Ser231Ala}-knockin mice were only partially resistant to the hypoglycaemic effect of AICAR, and glucose uptake was impaired in their EDL muscle only in response to the low concentration of AICAR (0.15 mmol/l) but not the high concentration of AICAR (2 mmol/l). Moreover, the *Tbc1d1*^{Ser231Ala}-knockin mutation did not impair contraction/exercise-stimulated glucose uptake in skeletal muscle (this study and Chen et al [27]), which is partially mediated by AMPK [9, 34]. One possible explanation is that other potential AMPK sites such as Thr^{499}, Ser^{621}, Ser^{660} and Ser^{700} on TBC1D1 [19, 36] might, together with Ser^{231}, account for the regulation of glucose uptake in response to the high concentration of AICAR (2 mmol/l) or muscle contraction. In support of this notion, overexpression of a TBC1D1-4P mutant (in which Ser^{231}, Thr^{499}, Thr^{590} and Ser^{621} were mutated to Ala) decreased contraction-stimulated glucose uptake in mouse skeletal muscle [20]. A second possibility is that the related RabGAP AS160 might contribute to AICAR- or contraction-stimulated glucose uptake. AICAR as well as muscle contraction could stimulate Ser^{595} phosphorylation of AS160, though its role in mediating AICAR- or contraction-stimulated glucose uptake remains to be established [22]. Third is the likelihood that factors other than TBC1D1 and AS160 might be responsible for muscle glucose uptake in response to the high concentration of AICAR (2 mmol/l) and muscle contraction. For example, guanine nucleotide exchange factors (GEFs) antagonise the effects of RabGAPs on activation of downstream Rabs, and can potentially regulate GLUT4 trafficking and glucose uptake. One such GEF, DENN/MADD domain containing 4C (Dennd4C), has recently been identified as an important factor in regulating GLUT4 trafficking in adipocytes [37]. It is conceivable that such GEFs also exist in muscle and regulate GLUT4 translocation in response to AICAR or muscle contraction. As the TBC1D1-Ser^{231} phosphorylation and/or its binding to 14-3-3s play only a moderate role in mediating AMPK-governed muscle glucose uptake, these knockin mice should be useful in helping to identify other putative mediators of AMPK-regulated muscle glucose uptake in the future.

A growing body of evidence shows that genetic manipulation or mutation of the related RabGAPs, TBC1D1 and AS160, regulates GLUT4 by modulating both its expression and translocation in a complex manner. Insulin-stimulated GLUT4 translocation to the plasma membrane was impaired in the *As160*^{Thr649Ala}-knockin mice, although expression of the transporter was elevated [25]. In contrast, expression of GLUT4 was decreased in various muscles and adipose tissue of the AS160-deficient mouse models [38–40] as well as in skeletal muscles from human patients who harbour a premature stop codon Arg^{684}Ter on AS160 [15]. Similarly, here we show that the *Tbc1d1*^{Ser231Ala}-knockin mutation did not affect GLUT4 expression but attenuated GLUT4 translocation to the plasma membrane in response to AICAR, whereas a natural TBC1D1-deficient mutant mouse and various *Tbc1d1*-knockout mice had reduced levels of GLUT4 in their skeletal muscle [14, 41–44]. Interestingly, the reduced GLUT4 levels in one of the *Tbc1d1*-knockout mouse models caused a decrease in exercise-stimulated glucose uptake in non-oxidative muscle fibres and consequently impaired exercise endurance [44]. It has been recently shown that the loss of AS160 GTPase-activating protein (GAP) activity accelerates lysosomal degradation of GLUT4 [40]. A key question remaining to be answered in all the TBC1D1 mouse models is whether the effects on GLUT4 translocation or expression depend on the GAP activity of TBC1D1.

In summary, the *Tbc1d1*^{Ser231Ala}-knockin mutation impacts on insulin-independent/AICAR-mediated whole-body glucose homeostasis in mouse at least in part through impairing muscle GLUT4 translocation and glucose uptake.

Acknowledgements We thank D. G. Hardie (University of Dundee, Dundee, UK) for the AMPKα1 and AMPKα2 antibodies, and G. Holman (University of Bath, Bath, UK) for the GLUT4 antibody.

Funding We thank the Ministry of Science and Technology of China (grant numbers 2014CB964704 and 2014BAI02B01 [National Key Scientific Research Program of China], grant number 2014AA021104 [National High Technology Research and Development Program of China]), the National Natural Science Foundation of China (grant numbers 31271498 and 31571211), the Ministry of Education of China (grant numbers 20120091120048 and NCET-13-0270) and the UK Medical Research Council (grant number U127084354) for financial support.

Contribution statement QLC, BXX, SSZ, PR, YS, SD, LC, CQ and ML performed the experiments, analysed the data and reviewed and edited the manuscript. KS and CM participated in the experimental design and reviewed and edited the manuscript. SC and HYW designed and performed the experiments, analysed the data and wrote the manuscript. All authors approved the final version of the manuscript. SC is the guarantor of this work.

Duality of interest KS is an employee of the Nestlé Institute of Health Sciences SA, Switzerland. All other authors declare that there is no duality of interest associated with their contribution to this manuscript.

References

1. Hardie DG, Ross FA, Hawley SA (2012) AMPK: a nutrient and energy sensor that maintains energy homeostasis. Nat Rev Mol Cell Biol 13:251–262
2. Richter EA, Ruderman NB (2009) AMPK and the biochemistry of exercise: implications for human health and disease. Biochem J 418:261–275

3. Steinberg GR, Kemp BE (2009) AMPK in health and disease. Physiol Rev 89:1025–1078
4. Kahn BB, Alquier T, Carling D, Hardie DG (2005) AMP-activated protein kinase: ancient energy gauge provides clues to modern understanding of metabolism. Cell Metab 1:15–25
5. Kurth-Kraczek EJ, Hirshman MF, Goodyear LJ, Winder WW (1999) 5′ AMP-activated protein kinase activation causes GLUT4 translocation in skeletal muscle. Diabetes 48:1667–1671
6. Viollet B, Andreelli F, Jorgensen SB et al (2003) The AMP-activated protein kinase alpha2 catalytic subunit controls whole-body insulin sensitivity. J Clin Invest 111:91–98
7. Jorgensen SB, Viollet B, Andreelli F et al (2004) Knockout of the alpha2 but not alpha1 5′-AMP-activated protein kinase isoform abolishes 5-aminoimidazole-4-carboxamide-1-beta-4-ribofuranosidebut not contraction-induced glucose uptake in skeletal muscle. J Biol Chem 279:1070–1079
8. Steinberg GR, O'Neill HM, Dzamko NL et al (2010) Whole body deletion of AMP-activated protein kinase β2 reduces muscle AMPK activity and exercise capacity. J Biol Chem 285:37198–37209
9. Mu J, Brozinick JT Jr, Valladares O, Bucan M, Birnbaum MJ (2001) A role for AMP-activated protein kinase in contraction- and hypoxia-regulated glucose transport in skeletal muscle. Mol Cell 7:1085–1094
10. Barnes BR, Marklund S, Steiler TL et al (2004) The 5′-AMP-activated protein kinase gamma3 isoform has a key role in carbohydrate and lipid metabolism in glycolytic skeletal muscle. J Biol Chem 279:38441–38447
11. Cho H, Mu J, Kim JK et al (2001) Insulin resistance and a diabetes mellitus-like syndrome in mice lacking the protein kinase Akt2 (PKB beta). Science 292:1728–1731
12. Dash S, Sano H, Rochford JJ et al (2009) A truncation mutation in TBC1D4 in a family with acanthosis nigricans and postprandial hyperinsulinemia. Proc Natl Acad Sci U S A 106:9350–9355
13. Stone S, Abkevich V, Russell DL et al (2006) TBC1D1 is a candidate for a severe obesity gene and evidence for a gene/gene interaction in obesity predisposition. Hum Mol Genet 15:2709–2720
14. Chadt A, Leicht K, Deshmukh A et al (2008) Tbc1d1 mutation in lean mouse strain confers leanness and protects from diet-induced obesity. Nat Genet 40:1354–1359
15. Moltke I, Grarup N, Jorgensen ME et al (2014) A common Greenlandic TBC1D4 variant confers muscle insulin resistance and type 2 diabetes. Nature 512:190–193
16. Sakamoto K, Holman GD (2008) Emerging role for AS160/TBC1D4 and TBC1D1 in the regulation of GLUT4 traffic. Am J Physiol Endocrinol Metab 295:E29–E37
17. Chen S, Synowsky S, Tinti M, MacKintosh C (2011) The capture of phosphoproteins by 14-3-3 proteins mediates actions of insulin. Trends Endocrinol Metab 22:429–436
18. Sano H, Kane S, Sano E et al (2003) Insulin-stimulated phosphorylation of a Rab GTPase-activating protein regulates GLUT4 translocation. J Biol Chem 278:14599–14602
19. Peck GR, Chavez JA, Roach WG et al (2009) Insulin-stimulated phosphorylation of the Rab GTPase-activating protein TBC1D1 regulates GLUT4 translocation. J Biol Chem 284:30016–30023
20. An D, Toyoda T, Taylor EB et al (2010) TBC1D1 regulates insulin- and contraction-induced glucose transport in mouse skeletal muscle. Diabetes 59:1358–1365
21. Ramm G, Larance M, Guilhaus M, James DE (2006) A role for 14-3-3 in insulin-stimulated GLUT4 translocation through its interaction with the RabGAP AS160. J Biol Chem 281:29174–29180
22. Geraghty KM, Chen S, Harthill JE et al (2007) Regulation of multisite phosphorylation and 14-3-3 binding of AS160 in response to IGF-1, EGF, PMA and AICAR. Biochem J 407:231–241
23. Chen S, Murphy J, Toth R, Campbell DG, Morrice NA, Mackintosh C (2008) Complementary regulation of TBC1D1 and AS160 by growth factors, insulin and AMPK activators. Biochem J 409:449–459
24. Pehmoller C, Treebak JT, Birk JB et al (2009) Genetic disruption of AMPK signaling abolishes both contraction- and insulin-stimulated TBC1D1 phosphorylation and 14-3-3 binding in mouse skeletal muscle. Am J Physiol Endocrinol Metab 297:E665–E675
25. Chen S, Wasserman DH, MacKintosh C, Sakamoto K (2011) Mice with AS160/TBC1D4-Thr649Ala knockin mutation are glucose intolerant with reduced insulin sensitivity and altered GLUT4 trafficking. Cell Metab 13:68–79
26. Ducommun S, Wang HY, Sakamoto K, MacKintosh C, Chen S (2012) Thr649Ala-AS160 knock-in mutation does not impair contraction/AICAR-induced glucose transport in mouse muscle. Am J Physiol Endocrinol Metab 302:E1036–E1043
27. Chen L, Chen Q, Xie B et al (2016) Disruption of the AMPK-TBC1D1 nexus increases lipogenic gene expression and causes obesity in mice via promoting IGF1 secretion. Proc Natl Acad Sci U S A 113:7219–7224
28. Nakada D, Saunders TL, Morrison SJ (2010) Lkb1 regulates cell cycle and energy metabolism in haematopoietic stem cells. Nature 468:653–658
29. Haldar M, Hancock JD, Coffin CM, Lessnick SL, Capecchi MR (2007) A conditional mouse model of synovial sarcoma: insights into a myogenic origin. Cancer Cell 11:375–388
30. Marcaletti S, Thomas C, Feige JN (2011) Exercise performance tests in mice. Curr Protoc Mouse Biol 1:141–154
31. Howlett KF, Andrikopoulos S, Proietto J, Hargreaves M (2013) Exercise-induced muscle glucose uptake in mice with graded, muscle-specific GLUT-4 deletion. Physiol Rep 1, e00065
32. Garcia-Roves PM, Osler ME, Holmstrom MH, Zierath JR (2008) Gain-of-function R225Q mutation in AMP-activated protein kinase gamma3 subunit increases mitochondrial biogenesis in glycolytic skeletal muscle. J Biol Chem 283:35724–35734
33. Lauritzen HP, Galbo H, Toyoda T, Goodyear LJ (2010) Kinetics of contraction-induced GLUT4 translocation in skeletal muscle fibers from living mice. Diabetes 59:2134–2144
34. O'Neill HM, Maarbjerg SJ, Crane JD et al (2011) AMP-activated protein kinase (AMPK) beta1beta2 muscle null mice reveal an essential role for AMPK in maintaining mitochondrial content and glucose uptake during exercise. Proc Natl Acad Sci U S A 108:16092–16097
35. Viollet B, Athea Y, Mounier R et al (2009) AMPK: lessons from transgenic and knockout animals. Front Biosci 14:19–44
36. Taylor EB, An D, Kramer HF et al (2008) Discovery of TBC1D1 as an insulin-, AICAR-, and contraction-stimulated signaling nexus in mouse skeletal muscle. J Biol Chem 283:9787–9796
37. Sano H, Peck GR, Kettenbach AN, Gerber SA, Lienhard GE (2011) Insulin-stimulated GLUT4 protein translocation in adipocytes requires the Rab10 guanine nucleotide exchange factor Dennd4C. J Biol Chem 286:16541–16545
38. Wang HY, Ducommun S, Quan C et al (2013) AS160 deficiency causes whole-body insulin resistance via composite effects in multiple tissues. Biochem J 449:479–489
39. Lansey MN, Walker NN, Hargett SR, Stevens JR, Keller SR (2012) Deletion of Rab GAP AS160 modifies glucose uptake and GLUT4 translocation in primary skeletal muscles and adipocytes and impairs glucose homeostasis. Am J Physiol Endocrinol Metab 303:E1273–E1286
40. Xie B, Chen Q, Chen L, Sheng Y, Wang HY, Chen S (2016) The Inactivation of RabGAP Function of AS160 promotes lysosomal degradation of glut4 and causes postprandial hyperglycemia and hyperinsulinemia. Diabetes. doi:10.2337/db16-0416
41. Dokas J, Chadt A, Nolden T et al (2013) Conventional knockout of Tbc1d1 in mice impairs insulin- and AICAR-stimulated glucose uptake in skeletal muscle. Endocrinology 154:3502–3514

42. Szekeres F, Chadt A, Tom RZ et al (2012) The Rab-GTPase-activating protein TBC1D1 regulates skeletal muscle glucose metabolism. Am J Physiol Endocrinol Metab 303:E524–E533
43. Hargett SR, Walker NN, Hussain SS, Hoehn KL, Keller SR (2015) Deletion of the Rab GAP Tbc1d1 modifies glucose, lipid, and energy homeostasis in mice. Am J Physiol Endocrinol Metab 309: E233–E245
44. Stockli J, Meoli CC, Hoffman NJ et al (2015) The RabGAP TBC1D1 plays a central role in exercise-regulated glucose metabolism in skeletal muscle. Diabetes 64:1914–1922